AGU PUBLICATIONS

Geophysical Research Letters

RESEARCH LETTER
10.1002/2014GL062380

Key Points:
- The 2012 warming terminated abruptly in autumn, which has been rarely observed
- The subtropical Pacific cooling plays a critical role in termination of warming
- The SSTA in the subtropical Pacific is an important factor for ENSO prediction

Supporting Information:
- Readme
- Figures S1–S4

Correspondence to:
J. Su,
sujz@cams.cma.gov.cn

Citation:
Su, J., B. Xiang, B. Wang, and T. Li (2014), Abrupt termination of the 2012 Pacific warming and its implication on ENSO prediction, *Geophys. Res. Lett.*, *41*, doi:10.1002/2014GL062380.

Received 31 OCT 2014
Accepted 20 NOV 2014
Accepted article online 25 NOV 2014

This is an open access article under the terms of the Creative Commons Attribution-NonCommercial-NoDerivs License, which permits use and distribution in any medium, provided the original work is properly cited, the use is non-commercial and no modifications or adaptations are made.

Abrupt termination of the 2012 Pacific warming and its implication on ENSO prediction

Jingzhi Su[1], Baoqiang Xiang[2,3], Bin Wang[4,5], and Tim Li[4,5]

[1]Chinese Academy of Meteorological Sciences, Beijing, China, [2]NOAA/Geophysical Fluid Dynamics Laboratory, Princeton, New Jersey, USA, [3]University Corporation for Atmospheric Research, Boulder, Colorado, USA, [4]International Pacific Research Center and Department of Meteorology, University of Hawaii, Honolulu, Hawaii, USA, [5]Earth System Modeling Center, Nanjing University of Information Science and Technology, Nanjing, China

Abstract In the summer of 2012, there was a clear signal of the developing El Niño over the equatorial Pacific, and many climate models forecasted the occurrence of El Niño with a peak phase in the subsequent winter. However, the warming was aborted abruptly in late fall. Here we show that the abrupt termination of the 2012 Pacific warming was largely attributed to the anomalous sea surface temperature (SST) cooling in the northeastern and southeastern subtropical Pacific. The anomalous SST cooling induced strong easterly and low-level divergence anomalies, suppressing the development of westerly and convection anomalies over the equatorial central Pacific. Thus, the surface warming over the equatorial Pacific was decoupled from the surface wind forcing and subsurface thermocline variability, inhibiting its further development into a mature El Niño in the winter of 2012–2013. This study highlights the importance of the SST anomaly in the subtropical Pacific in El Niño prediction.

1. Introduction

Understanding and improving El Niño/Southern Oscillation (ENSO) prediction are critical for seasonal predictions because ENSO provides the most important predictability source for global atmosphere [e.g., *McPhaden et al.,* 2006]. The current ENSO prediction skill is usually high at about six months [e.g., *Jin et al.,* 2008]. For longer time lead forecast above 6 months, the forecast skill is relatively low [e.g., *Cane et al.,* 1986; *Fedorov et al.,* 2003], which is mainly attributed to the spring predictability barrier [*Webster and Yang*, 1992]. Some recent studies showed that the performance of ENSO prediction can be one year [*Ludescher et al.,* 2013] or even two years for some strong El Niño events [*Luo et al.,* 2008], while the ENSO prediction is challenged by the limitation of the dynamical models to distinguish the eastern Pacific and central Pacific ENSOs at 4–6 months lead time [*Hendon et al.,* 2009; *Jeong et al.,* 2012].

There are no ENSO cases that are exactly the same from the historical observations. In this study, we are focusing on the tropical Pacific warming of the year 2012, which actually failed to develop into a real "El Niño" due to its sudden decay in boreal summer and fall. During the summer of 2012, the eastern Pacific SST anomaly exceeded a maximum of above 1°C. Interestingly, most of current state-of-the-art climate models predicted the occurrence of a modest El Niño in the winter of 2012–2013 given the observed initial warming in summer [http://www.cpc.ncep.noaa.gov/products/NMME/]. It turned out to be a false alarm of El Niño. Thus, the 2012 summer warming was a rarely abnormal case with unexpected termination. Understanding what conditions prevented the development of the equatorial Pacific warming in the following fall and winter is essential to improve our understanding of ENSO dynamics as well as ENSO prediction.

2. Data and Methods

We use several monthly mean data sets, including wind data from European Centre for Medium-Range Weather Forecasts (ECMWF) ERA-Interim data set [*Dee et al.,* 2011], precipitation from Global Precipitation Climatology Project (GPCP) v2.2 [*Adler et al.,* 2003], and SST from National Oceanic and Atmospheric Administration (NOAA) ERSST (Extended Reconstructed Sea Surface Temperature SST, V3b) [*Smith et al.,* 2008]. To reduce the data uncertainty, we use two ocean reanalysis data and three heat flux data sets. The ocean reanalysis data sets are from GODAS (Global Ocean Data Assimilation System) [*Saha et al.,* 2006] and the ensemble coupled data assimilation (ECDA) version 3.1 of Geophysical Fluid Dynamics Laboratory (GFDL)

©2014. The Authors.

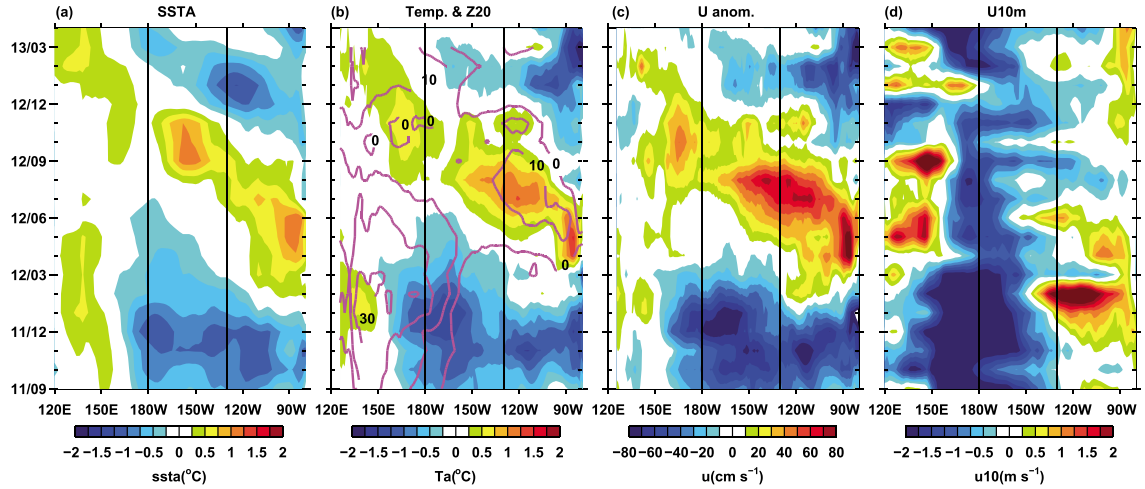

Figure 1. The evolution of (a) sea surface temperature anomalies (SSTAs) from Extended Reconstructed Sea Surface Temperature SST (ERSST), (b) mixed layer temperature anomalies (shading) and thermocline depth anomalies (contour line) from Global Ocean Data Assimilation System (GODAS) and ensemble coupled data assimilation (ECDA), (c) zonal ocean current anomalies from GODAS and ECDA, and (d) anomalous zonal wind at 10 m along the equator (within 5°N–5°S). The wind fields are from REA-interim. Two solid lines denote the zonal location of the central equatorial Pacific (CP; 180°W–130°W), and eastern equatorial Pacific sections (EP; 130°W–80°W).

[*Chang et al.,* 2013]. The surface heat flux data are from National Centers for Environmental Prediction (NCEP) of NCEP-1 and NCEP-2, and Woods Hole Oceanographic Institution (WHOI) Objectively Analyzed Air-Sea Fluxes (OAFlux) [*Yu et al.,* 2008]. The climatological mixed layer depth from French Research Institute for Exploitation of the Sea with a fixed threshold criterion (0.03 kg m^{-3}) [*de Boyer Montégut et al.,* 2004] is used to define the mixed layer depth.

For convenience, the equatorial (5°S–5°N) Pacific is divided into three sections: the western equatorial Pacific (west to 180°W), the central equatorial Pacific (CP; 180°W–130°W), and the eastern equatorial Pacific sections (EP; 130°W–80°W). The period of 1980–2012 is used to calculated climatological mean values.

3. Results

3.1. Observational Features of the Aborted El Niño in 2012

We first examine the observational evolution of the anomalous SST, zonal wind, and thermocline depth over the equatorial Pacific (Figure 1). Following the La Niña event in 2011, the negative SST anomalies (SSTAs) persisted in the first half year of 2012 in the CP (Figure 1a). In the EP, positive SSTAs appeared at around February 2012 and reached above 0.5°C during boreal spring (March–May) of 2012. Note that the positive SSTAs were mainly confined in the region east of 140°E before June 2012, which then extended westward to the CP. During the mid- to late-summer, the maximum positive SSTAs reached about 1.0°C both in the CP and EP. Intriguingly, the positive SSTAs decayed rapidly from late summer (fall) for the EP (CP), representing an abrupt termination of El Niño. As a result, the SSTAs in the equatorial Pacific during the winter of 2012–2013 appeared to be a rather neutral condition. Consistently, the ocean reanalysis data also well capture the observational evolution feature (Figure 1b). In the following subsection, we will investigate the dynamics controlling the SSTAs evolution in 2012 in the CP and EP, particularly focusing on the mechanisms resulting in the abrupt termination of the warming.

3.2. Understanding the Pacific Warming Development in 2012

To identify the factors governing the SSTAs evolution, a mixed layer heat budget analysis following *Su et al.* [2010] was carried out in the CP region and EP region, respectively. The mixed layer depth for the EP and CP region is from the climatological values [*de Boyer Montégut et al.,* 2004]. The heat budgets were calculated based on individual data separately and the ensemble values (GODAS and ECDA) are analyzed in the following. For convenience, the SSTAs evolution periods are separated into the developing phase and decaying phase. According to the observed SSTAs, the developing phase is February–June (February–August) 2012 for the EP (CP) region, and the decaying phase is July–November (September–November) 2012 for the EP (CP) region.

©2014. The Authors.

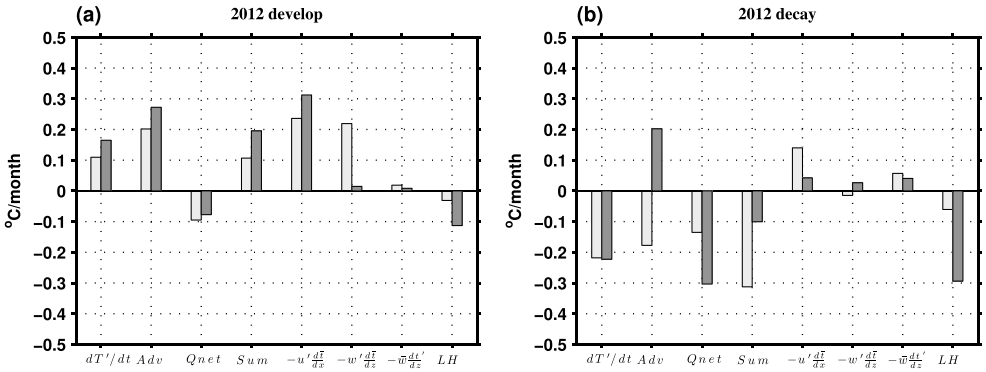

Figure 2. (a) The mixed-layer temperature tendency and budget analysis for the developing phase of the 2012 warming event in the EP (gray) and CP (black): the observed temperature tendency, the three-dimensional temperature advection, the surface flux heating, the sum of the advection and the surface heat flux, the three terms of temperature advection, and the latent flux. The calculation is based on GODAS and ECDA. The heat fluxes are from NCEP1, NCEP2, and OAFlux. (b) Same as Figure 2a, but for decaying phase of 2012 warming even. The decaying phases for the EP and CP are during July–November and September–November, respectively. The capital terms represent climatological annual cycle, and the prime terms represent anomalies.

All the terms of the heat budget are shown in Figure S1, and some relatively important terms are shown in Figure 2. In the following, $\boldsymbol{V}=(\boldsymbol{u},\boldsymbol{v},\boldsymbol{w})$ represents the three-dimensional ocean current, $\nabla=(\partial/\partial\boldsymbol{x},\partial/\partial\boldsymbol{y},\partial/\partial\boldsymbol{z})$ denotes the three-dimensional gradient operator, a prime (′) represents the anomaly variables, and a bar ($\bar{}$) represents the climatologic annual cycle variables. It is indicated that the residual term is relatively small during the developing phase but relatively larger over the decaying phase (but qualitatively consistent) (Figure 2).

As mentioned above, the initial warming occurred first in the EP in around February 2012 (Figure 1a). During February–July of 2012, there were anomalous downwelling in the EP region (Figures 3a–3c), which is linked to the anomalous westerlies over the EP (Figure 1d). Hence, the anomalous vertical advection term associated with the mean vertical temperature gradient became positive $\left(-w'\ \partial\overline{T}/\partial z>0\right)$, which was largely responsible for the initial SST warming (Figure 2a) and also the subsurface warming after April–May (Figure 3). Besides, the

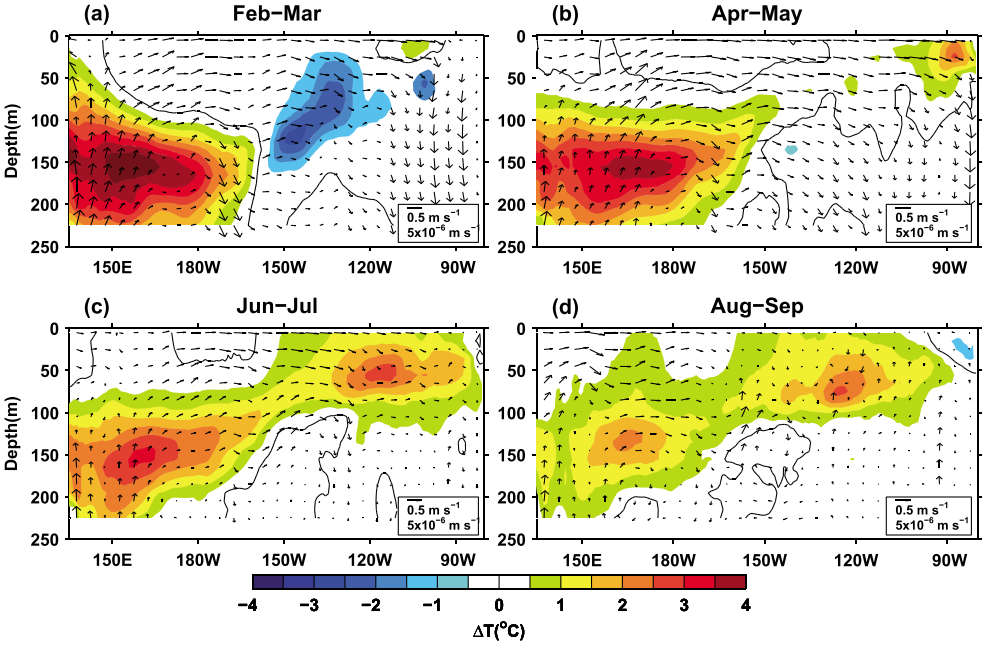

Figure 3. Mean temperature anomalies (contour, with intervals of 0.5°C) and ocean zonal and vertical current (vectors) along the equator (averaged within 2°N–2°S) during 2012. The data are from GODAS and ECDA.

©2014. The Authors.

subsurface temperature anomalies in the EP region could be affected by the eastward propagation of the positive thermocline depth (Z20) anomalies from the western Pacific, which were accumulated there during the decaying phase of the La Niña of 2011. The positive Z20 anomalies in the EP region enhanced the local SST warming through the positive thermocline feedback after April 2012 ($-\overline{w}\ \partial T'/\partial z > 0$; Figure 2a).

The SST warming in the EP region was further enhanced by the positive zonal advection term ($-u'\ \partial\overline{T}/\partial x > 0$; Figure 2a) because of the anomalous eastward currents ($u' > 0$; Figure 3). Following *Su et al.* [2010], the anomalous zonal currents are separated into the geostrophic components associated with thermocline change and the local wind-driven ageostrophic currents. The mean simulated zonal ocean current anomalies (0.22 m s^{-1}) in the EP region were dominantly controlled by the zonal geostrophic component (0.22 m s^{-1}) rather than the local wind-driven component (0.01 m s^{-1}) (Figure S2a).

After the initiation of the SST warming in the EP, it expanded westward with the most pronounced warming over the CP (Figure 1a). It is revealed that the positive SSTAs tendency in the CP region was mainly determined by the zonal advection term ($-u'\ \partial\overline{T}/\partial x > 0$; Figure 2a). Similarly, the positive zonal ocean current anomalies (0.16 m s^{-1}) were contributed mostly by the eastward geostrophic currents (Figure S2a), which were induced by the equatorial deepened thermocline. Due to the weak thermocline change over the CP, the thermocline feedback was very weak during both the developing and decaying phases (Figure 2).

3.3. Cause of the Abrupt Termination of the 2012 Pacific Warming

In this subsection, we are focusing on revealing what induces the rapid decay of the SST warming for both the EP (from the late summer) and CP (from the fall). Theoretically, the warming decay could be linked to the reduction of positive feedbacks and/or the increase of negative feedbacks. As shown in Figure 2b, the negative SSTAs tendency in the EP was primarily determined by the ocean advection terms and the negative surface heat flux.

By contrast, the negative SSTAs tendency in the CP region was mainly caused by the negative net surface heat flux anomalies (Figure 2b). The net heat flux anomalies became negative (about -0.3°C $month^{-1}$) from September 2012, which was the major contributor for the negative SSTAs tendency there. At the same time, the major positive feedback (zonal advection feedback) during the developing phase was reduced significantly. It was shown that the ENSO amplitude usually tends to decay rapidly if the positive feedbacks (thermocline feedback and zonal advection feedback) are weak because of the strong thermodynamic (surface heat flux) damping effect [*Jin et al.,* 2006; *Xiang et al.,* 2012]. The intensified negative net heat fluxes (mainly the latent heat flux) were caused by the SST warming and also the enhanced trade winds (Figure 4). Examination of the two major positive feedback terms (zonal advection feedback and thermocline feedback) shows that they are still positive but with much smaller amplitude compared to that in the developing phase. Hence, the negative SST tendency for both the CP and EP reflected the combined effect of the intensified negative feedback (thermal damping) and weakened positive feedback (zonal advection feedback) compared to the developing phase.

The above budget analysis provides some clues for the rapid SSTAs decay but fails to offer the root cause. As a strong atmosphere-ocean coupled mode, the conventional El Niño is usually characterized by anomalous westerly winds in the western equatorial Pacific, deepened thermocline depth, and anomalous convection near the CP. This coupled mode can be sustained and intensified through the positive Bjerknes feedback [*Bjerknes*, 1969]. However, the 2012 El Niño-like warming case exhibited a distinctly different atmosphere-ocean pattern in comparison to the conventional El Niño events. Our analyses show that the termination of the SST warming in the central-eastern equatorial Pacific was tightly linked to the SST cooling in the northeastern and southeastern subtropical Pacific (STP) (Figure 4). Previous studies have documented that the SSTAs in the northeastern/southeastern subtropical Pacific play an important role in triggering the equatorial SST variability [*Vimont et al.,* 2001; *Chiang and Vimont*, 2004; *Yu et al.,* 2010; *Ham et al.,* 2013; *Zhang et al.,* 2014].

The negative SSTAs in the northeastern STP persisted from the previous 2010–2011 La Niña (not shown) and lasted through almost the whole year of 2012 (Figure 4). Associated with this SST cooling in the northeastern STP, the suppressed precipitation was found near the Intertropical Convergence Zone (ITCZ) region that drove a local cyclonic circulation and anomalous easterly wind near the equator. Meanwhile, through the wind-evaporation-SST feedback [*Xie and Philander,* 1994], the cold SSTAs can sustain itself and even penetrate into the equatorial western Pacific [*Chiang and Vimont*, 2004; *Vimont et al.,* 2001; *Ashok et al.,* 2012] and then force the easterly wind anomalies over the equatorial Pacific. With the existence of the forced

©2014. The Authors.

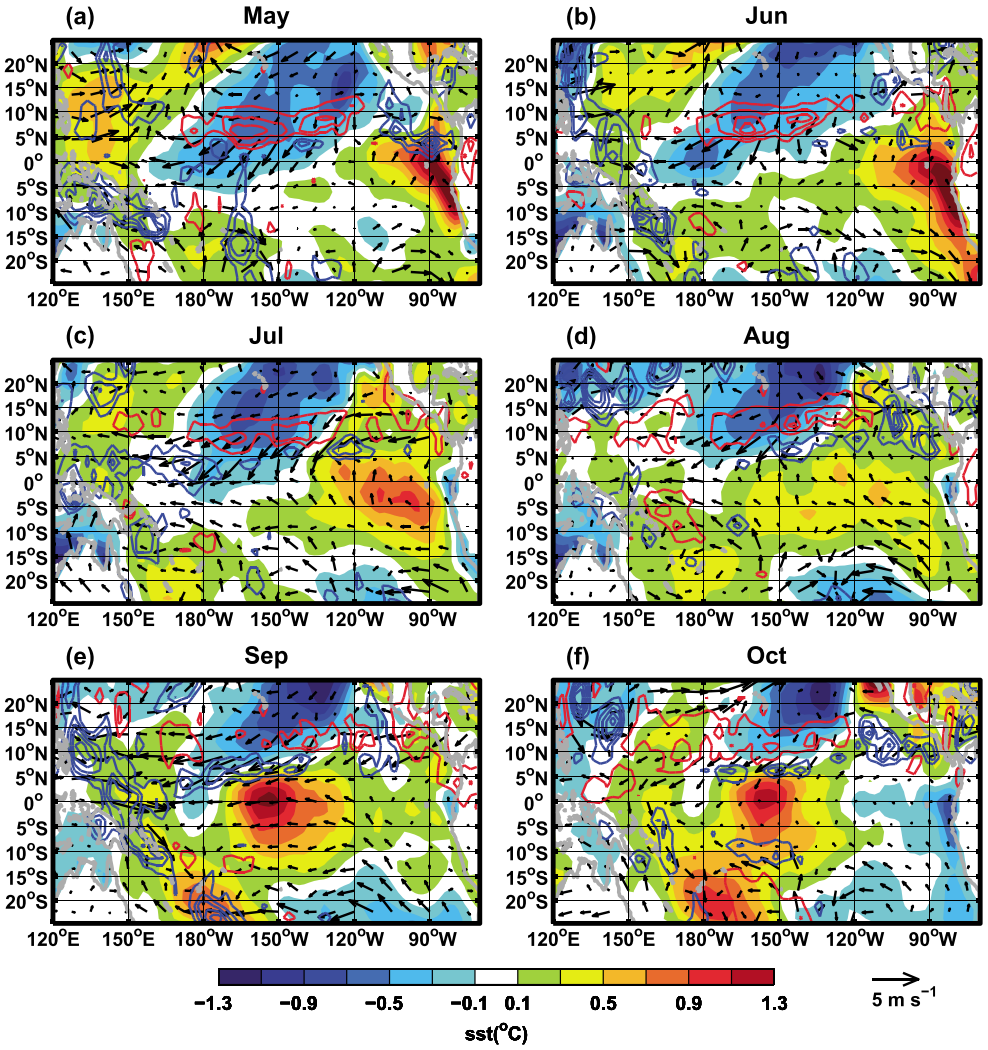

Figure 4. The SSTAs (shading, with intervals of 0.2°C), the anomalous precipitation (contours, blue for positive and red for negative, with intervals of 2 mm d^{-1}), and the anomalous wind at 10 m (vector, in m s^{-1}) during each month of 2012.

easterly wind anomalies over the central-to-western Pacific, the CP shows a low-level divergence inhibiting the development of anomalous convection and westerly wind anomalies associated with the EP warming [*Xiang et al.,* 2013]. Meanwhile, the easterly wind anomalies can excite the upwelling oceanic Kelvin wave propagating eastward and then cancel or reduce the thermocline depth change anomalies in the CP, which then reduce the zonal advection feedback (Figure S1b) because of the reduction of eastward geostrophic currents (Figure S2b).

In the EP region, anomalous easterlies appeared around July 2012 and were strengthened in August–September (Figure 1d), which were likely associated with negative SSTAs in the southern STP (around 130°W–90°W) through the wind-evaporation-SST feedback [*Zhang et al.,* 2014]. The local easterly wind anomalies also contributed to the warming decay by increasing latent heat flux and vertical cold advection (Figure S1) through generating anomalous upwelling, which tends to occur readily near the coast of Southern American (Figure 3d). Since the negative SSTAs came into being first in the far eastern equatorial Pacific (Figures 4d–4f), there was zonal cold advection during decaying period in EP ($-\bar{u}\ \partial T'/\partial x < 0$; Figure S1b) with the aid of westward mean ocean currents. The anomalous cooling waters were also transported poleward by the mean meridional currents, generating negative meridional advection $\left(-\bar{v}\ \partial T'/\partial y < 0;\ \text{Figure S1b}\right)$.

Therefore, we conclude that the easterly wind anomalies decoupled the surface warming from the convection and the thermocline variability, holding the key for the termination of the 2012 Pacific warming event.

©2014. The Authors.

4. Summary and Discussion

After 1980s, most of El Niño events were initiated from the CP. Here we show that the onset of an "El Niño-like" warming event in 2012 occurred in the EP during spring with its warming expanding westward to the CP during the following summer. It was expected to develop into a mature El Niño in the following winter according to the current operational model forecasts. However, the positive SSTAs were abruptly terminated in boreal fall so that a neutral condition was observed in the winter of 2012–2013. We conclude that the abrupt termination of 2012 warming was mainly controlled by the anomalous SST cooling in the subtropical Pacific, which decoupled the equatorial SST warming from convection, wind, and oceanic subsurface variability over the equatorial Pacific.

One question may arise concerning the failure of forecasts by the state-of-the-art models in the summer 2012: What factors hinder the forecasting ability? Here, we notice that the forecasting ability is likely related to the initial conditions, particularly the negative SSTAs in the eastern subtropical Pacific [http://www.cpc.ncep.noaa.gov/products/NMME/]. Although most models failed in forecasting 2012 warming, the CFSv1 model still forecasted a neutral or negative state in the equatorial Pacific for the winter 2012 (Figure S3). One outstanding difference between the CFSv1 and other models lies in the initial conditions: There were significant negative SSTAs in the northeastern subtropical Pacific in the CFSv1, while such negative SSTAs were relatively weak in other models (Figure S3). Such features imply that the SSTAs in the northeastern subtropical Pacific may affect the evolution of equatorial warming in the climate models. This process highlights the significant role of the SSTAs in the subtropical Pacific in controlling the El Niño evolution.

In fact, the termination of 2012 Pacific warming is not a unique case. For example, similar processes can also be found in the SSTAs evolution in the year of 2008 (Figure S4), during which the termination of SST warming in the eastern equatorial Pacific tends to be related with the negative SSTAs in the subtropical Pacific. Since the SSTAs in the subtropical Pacific persist from previous winter, the relative longer lead time may facilitate the prediction of El Niño events. Hence, the SSTAs in the subtropical Pacific can be an important predictor which should be considered in the future prediction of ENSO as well as seasonal climate prediction.

Acknowledgments

Comments from the two anonymous reviewers were helpful to improving the paper. This research was founded by China National 973 project 2015CB453200, the National Natural Science Foundation of China (under Grant 41221064 and 41376020), and the International S&T Cooperation Project of the Ministry of Science and Technology of China under Grant 2009DFA21430. BX was supported by NOAA MAPP Program under Awards NA12OAR4310075. TL acknowledged the support of ONR grant N00014-1210450. This is the ESMC publication 24.

The Editor thanks two anonymous reviewers for their assistance in evaluating this paper.

References

Adler, R. F., et al. (2003), The Version 2 Global Precipitation Climatology Project (GPCP) Monthly Precipitation Analysis (1979-present), *J. Hydrometeorol.*, *4*, 1147–1167.

Ashok, K., T. P. Sabin, P. Swapna, and R. G. Murtugudde (2012), Is a global warming signature emerging in the tropical Pacific?, *Geophys. Res. Lett.*, *39*, L02701, doi:10.1029/2011GL050232.

Bjerknes, J. (1969), Atmospheric teleconnections from the equatorial Pacific, *Mon. Weather Rev.*, *97*, 163–172.

Cane, M. A., S. E. Zebiak, and S. C. Dolan (1986), Experimental forecasts of El Niño, *Nature*, *321*, 827–832.

Chang, Y.-S., S. Q. Zhang, A. Rosati, T. L. Delworth, and W. F. Stern (2013), An assessment of oceanic variability for 1960–2010 from the GFDL ensemble coupled data assimilation, *Clim. Dyn.*, *40*, 775–803.

Chiang, J. C. H., and D. J. Vimont (2004), Analogous Pacific and Atlantic meridional modes of tropical atmosphere–ocean variability, *J. Clim.*, *17*, 4143–4158.

de Boyer Montégut, C., G. Madec, A. S. Fischer, A. Lazar, and D. Iudicone (2004), Mixed layer depth over the global ocean: An examination of profile data and a profile-based climatology, *J. Geophys. Res.*, *109*, C12003, doi:10.1029/2004JC002378.

Dee, D. P., et al. (2011), The ERA-Interim reanalysis: Configuration and performance of the data assimilation system, *Q. J. R. Meteorol. Soc.*, *137*, 553–597.

Fedorov, A. V., S. L. Harper, S. G. Philander, B. Winter, and A. Wittenberg (2003), How predictable is El Niño?, *Bull. Am. Meteorol. Soc.*, *84*, 911–919.

Ham, Y.-G., J.-S. Kug, J.-Y. Park, and F.-F. Jin (2013), Sea surface temperature in the north tropical Atlantic as a trigger for El Niño/Southern Oscillation events, *Nat. Geosci.*, *6*, 112–116, doi:10.1038/ngeo1686.

Hendon, H. H., E. Lim, G. Wang, O. Alves, and D. Hudson (2009), Prospects for predicting two flavors of El Niño, *Geophys. Res. Lett.*, *36*, L19713, doi:10.1029/2009GL040100.

Jeong, H.-I., D.-Y. Lee, K. Ashok, J.-B. Ahn, J.-Y. Lee, J.-J. Luo, J.-K. E. Schemm, H. H. Hendon, K. Braganza, and Y.-G. Ham (2012), Assessment of the APCC coupled MME suite in predicting the distinctive climate impacts of two flavors of ENSO during boreal winter, *Clim. Dyn.*, *39*, 475–493, doi:10.1007/s00382-012-1359-3.

Jin, E. K., et al. (2008), Current status of ENSO prediction skill in coupled ocean atmosphere models, *Clim. Dyn.*, *31*, 647–664, doi:10.1007/s00382-008-0397-3.

Jin, F.-F., S. T. Kim, and L. Bejarano (2006), A coupled stability index for ENSO, *Geophys. Res. Lett.*, *33*, L23708, doi:10.1029/2006GL027221.

Ludescher, J., A. Gozolchiani, M. I. Bogachev, A. Bunde, S. Havlin, and H. J. Schellnhuber (2013), Improved El Niño forecasting by cooperativity detection, *Proc. Natl. Acad. Sci. U.S.A.*, *110*, 11,742–11,745, doi:10.1073/pnas.1309353110.

Luo, J.-J., S. Masson, S. K. Behera, and T. Yamagata (2008), Extended ENSO predictions using a fully coupled ocean–atmosphere model, *J. Clim.*, *21*, 84–93.

McPhaden, M. J., S. E. Zebiak, and M. H. Glantz (2006), ENSO as an integrating concept in earth science, *Science*, *314*, 1740–1745, doi:10.1126/science.1132588.

Saha, S., et al. (2006), The NCEP Climate Forecast System, *J. Clim.*, *19*, 3483–3517.

Smith, T. M., R. W. Reynolds, T. C. Peterson, and J. Lawrimore (2008), Improvements to NOAA's historical merged land–ocean surface temperature analysis (1880–2006), *J. Clim.*, *21*, 2283–2296.

©2014. The Authors.

Su, J., R. Zhang, T. Li, X. Rong, J.-S. Kug, and C.-C. Hong (2010), Causes of the El Niño and La Niña amplitude asymmetry in the Equatorial Eastern Pacific, *J. Clim.*, *23*, 605–617.

Vimont, D. J., D. S. Battisti, and A. C. Hirst (2001), Footprinting: A seasonal link between the mid-latitudes and tropics, *Geophys. Res. Lett.*, *28*, 3923–3926, doi:10.1029/2001GL013435.

Webster, P. J., and S. Yang (1992), Monsoon and ENSO: Selectively interactive systems, *Q. J. R. Meteorol. Soc.*, *118*, 877–926.

Xiang, B., B. Wang, Q. Ding, F.-F. Jin, X. Fu, and H.-J. Kim (2012), Reduction of the thermocline feedback associated with mean SST bias in ENSO simulation, *Clim. Dyn.*, *39*(6), 1413–1430, doi:10.1007/s00382-011-1164-4.

Xiang, B., B. Wang, and T. Li (2013), A new paradigm for the predominance of standing central Pacific warming after the late 1990s, *Clim. Dyn.*, *41*(2), 327–340, doi:10.1007/s00382-012-1427-8.

Xie, S.-P., and S. G. H. Philander (1994), A coupled ocean–atmosphere model of relevance to the ITCZ in the eastern Pacific, *Tellus, Ser. A*, *46*, 340–350.

Yu, J.-Y., H.-Y. Kao, and T. Lee (2010), Subtropics-related interannual sea surface temperature variability in the central equatorial Pacific, *J. Clim.*, *23*, 2869–2884.

Yu, L., X. Jin, and R. A. Weller (2008), Multidecade Global Flux Datasets from the Objectively Analyzed Air-sea Fluxes (OAFlux) Project: Latent and sensible heat fluxes, ocean evaporation, and related surface meteorological variables, *Rep. OA-2008-1*,64 pp., Woods Hole Oceanogr. Inst., Woods Hole, Mass.

Zhang, H., C. Deser, A. C. Clement, and R. Tomas (2014), Equatorial signatures of the Pacific Meridional Modes: Dependence on mean climate state, *Geophys. Res. Lett.*, *41*, 568–574, doi:10.1002/2013GL058842.

©2014. The Authors.